Superconductivity of the topological insulator Bi_2Se_3 at high pressure

2013 J. Phys.: Condens. Matter 25 362204

(http://iopscience.iop.org/0953-8984/25/36/362204)

OPEN ACCESS
IOP PUBLISHING

IOP FTC
JOURNAL OF PHYSICS: CONDENSED MATTER

J. Phys.: Condens. Matter **25** (2013) 362204 (5pp)
doi:10.1088/0953-8984/25/36/362204

FAST TRACK COMMUNICATION

Superconductivity of the topological insulator Bi_2Se_3 at high pressure

P P Kong[1], J L Zhang[1], S J Zhang[1], J Zhu[1], Q Q Liu[1], R C Yu[1], Z Fang[1], C Q Jin[1], W G Yang[2], X H Yu[1,3], J L Zhu[1,3] and Y S Zhao[1,3]

[1] Beijing National Laboratory for Condensed Matter Physics, and Institute of Physics, Chinese Academy of Sciences, Beijing, 100190, People's Republic of China
[2] High Pressure Synergetic Consortium (HPSynC) and High Pressure Collaborative Access Team (HPCAT), Geophysical Laboratory, Carnegie Institution of Washington, Argonne, IL 60439, USA
[3] Los Alamos Neutron Science Center (LANSCE), Los Alamos National Laboratory, Los Alamos, NM 87545, USA

E-mail: Jin@iphy.ac.cn

Received 23 May 2013, in final form 4 July 2013
Published 14 August 2013
Online at stacks.iop.org/JPhysCM/25/362204

Abstract
The pressure-induced superconductivity and structural evolution of Bi_2Se_3 single crystals are studied. The emergence of superconductivity at an onset transition temperature (T_c) of about 4.4 K is observed at around 12 GPa. T_c increases rapidly to a maximum of 8.2 K at 17.2 GPa, decreases to around 6.5 K at 23 GPa, and then remains almost constant with further increases in pressure. Variations in T_c with respect to pressure are closely related to the carrier density, which increases by over two orders of magnitude from 2 to 23 GPa. High-pressure synchrotron radiation measurements reveal structural transitions at around 12, 20, and above 29 GPa. A phase diagram of superconductivity versus pressure is also constructed.

(Some figures may appear in colour only in the online journal)

Topological insulators (TIs), which feature a bulk band gap but gapless edge state protected by time-reversal symmetry, are a new frontier in condensed matter physics and have thus attracted significant research interest worldwide [1–8]. Many useful applications are expected from topological compounds, ranging from novel research on Majorana fermions to prospective applications in topological computers [9] to exotic topological superconductors. Recently, the group of three-dimensional TIs Bi_2Te_3, Bi_2Se_3, etc, was predicted, and the conducting surface states with Dirac cones were confirmed by angle-resolved photoemission spectroscopy (ARPES) [4, 7, 10, 11].

Similar to TIs, topological superconductors have a full pairing gap in the bulk and gapless edge states consisting of elusive Majorana fermions [12]. When TIs are combined with magnetic or superconducting materials, the Majorana state may be realized at their interfaces. Several applications [10, 13, 14] of interfaces between TIs and superconductors have been proposed. The superconductivity of Bi_2Se_3 has been observed by copper intercalation in van der Waals gaps between quintuple layers [15], while Bi_2Te_3 is known to become superconductive at pressures above 3 GPa [16]. Pressure is effective in generating or tuning superconductivity by modifying the electronic structure through directly changing interatomic distances without introducing defects or impurities. In this study, we report the effects of pressure on Bi_2Se_3. We found that Bi_2Se_3 becomes superconducting at its high-pressure phases.

Bi_2Se_3 single crystals were grown by the Bridgman method, the details of which are described in [16]. High-purity Bi (99.999%) and Se (99.999%) were mixed at a molar ratio of 2:3, ground, pressed into pellets, and then loaded into a

quartz Bridgman ampule, which was subsequently evacuated and sealed. The ampule was placed in a furnace and heated to 800 °C for two days, before being slowly cooled down at a rate of 3 °C h^{-1} to 550 °C. The ampule was then kept for three days and allowed to slowly cool down to room temperature. The product was cleaved easily along the basal plane. Bi_2Se_3 single crystals were ground to powder for x-ray powder diffraction (XRD) measurements.

The resistance of Bi_2Se_3 single crystals was measured at high pressure using the standard four-probe method in a diamond anvil cell (DAC) made up of CuBe alloy as described in [16, 17]. The diamond culet was about 500 μm in diameter. A gasket made of T301 stainless steel was preindented from a thickness of 250 μm to 60 μm, and drilled with a center hole diameter of 250 μm. Fine cubic boron nitride (cBN) powder was used to cover the gasket to keep the electrode leads insulated from the metallic gasket. The cBN powder was pressed and further drilled into a center hole with a diameter of 100 μm to serve as a sample chamber into which a Bi_2Se_3 single crystal with dimensions of 70 μm × 70 μm × 10 μm was inserted with soft hexagonal boron nitride (hBN) fine powder surrounding it as a pressure-transmitting medium that can provide a good quasi-hydrostatic pressure environment. Slim gold wires of 18 μm diameter were used as electrodes. Pressure was determined by the ruby fluorescence method [18, 19]. The DAC was placed inside a MagLab system to perform the experiments. To ensure equilibrium, the MagLab system automatically controlled the temperature so that temperature slowly decreased. A thermometer located near the diamond in the DAC accurately measured sample temperature. The Hall coefficient at high pressure was measured using the van der Pauw method.

XRD measurements with synchrotron radiation at high pressure and low temperature were performed using a symmetrical Mao Bell DAC at the High Pressure Collaborative Access Team (HPCAT) of the Advanced Photon Source of Argonne National Laboratory. The wavelength used was 0.398 Å. The two-dimensional image plate patterns obtained were converted to one-dimensional 2θ versus intensity data using the Fit2D software package.

Bi_2Se_3, the structure of which is identical to that of Bi_2Te_3, has a nearly ideal single Dirac cone in its surface state and the largest bulk energy gap (approximately 0.3 eV) among all known 3D TIs [6, 7]. It is a direct gap semiconductor [13], but strong spin–orbit coupling inverts the bulk bands at the Γ point [6]. Several reports on the effects of pressure on Bi_2Se_3 have been published [20, 21]. In this study, we measured the changes in transport properties of Bi_2Se_3 single crystals in a DAC with increasing pressure. The carrier density of Bi_2Se_3 single crystals is around 2 × 10^{18} cm^{-3} at ambient pressure and 30 K.

Figure 1 represents the temperature dependence of the *a*–*b* plane resistance at different pressures. The pressure was monotonically increased. Figure 1(a) shows the temperature dependence of resistance in the low-pressure phase with small pressure intervals. When the pressure is below 3.1 GPa, Bi_2Se_3 displays weak metallic behavior. It becomes more metallic above 5.1 GPa, which is probably related to the

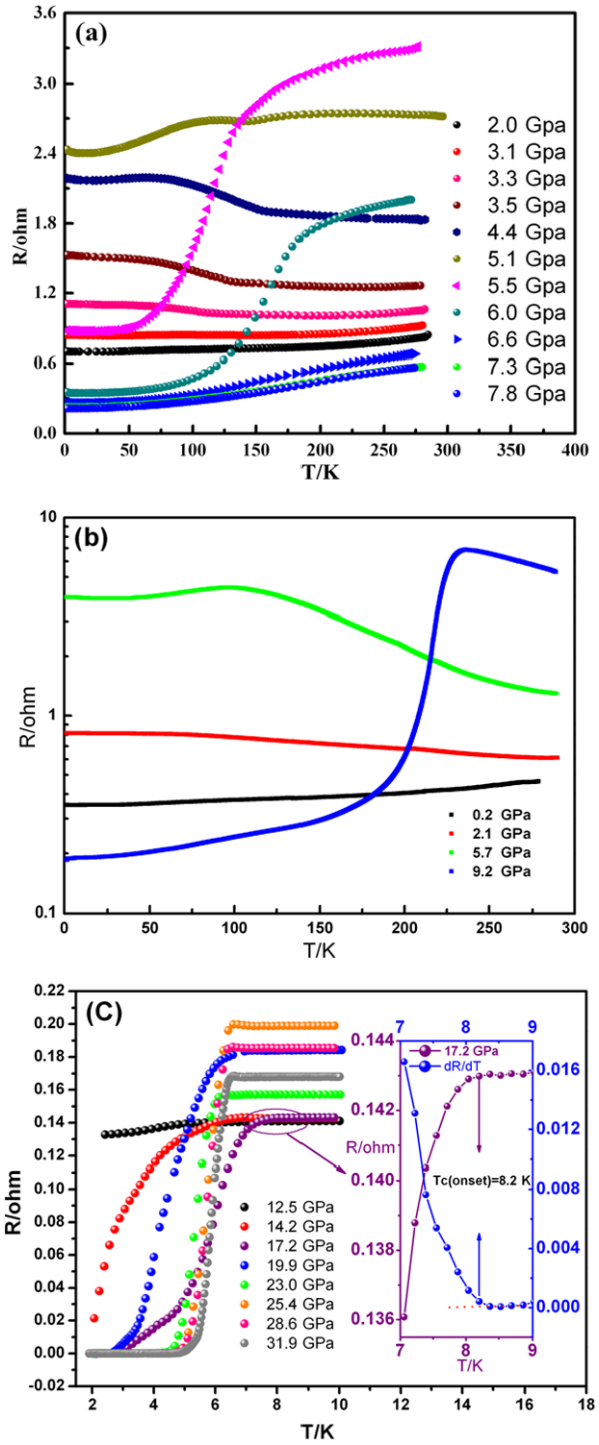

Figure 1. Resistance of Bi_2Se_3 single crystals as a function of temperature in the low-pressure phase (LPP): (a) with the small pressure intervals of the first experiment, (b) with large pressure intervals from another experiment, and (c) high-pressure phases showing superconductivity. The first superconducting pressure is around 12 GPa. The inset is an enlargement of resistance versus temperature around the superconducting region at 17.2 GPa; the differential of resistance over temperature (dR/dT) shows the onset transition temperature (8.2 K) (the red dash–dot line is a guide to the eye).

pressure-induced electronic topological transition (ETT) in Bi_2Se_3 near 5 GPa, as previously reported [21]. The changes in the behavior of the samples in the low-pressure phase

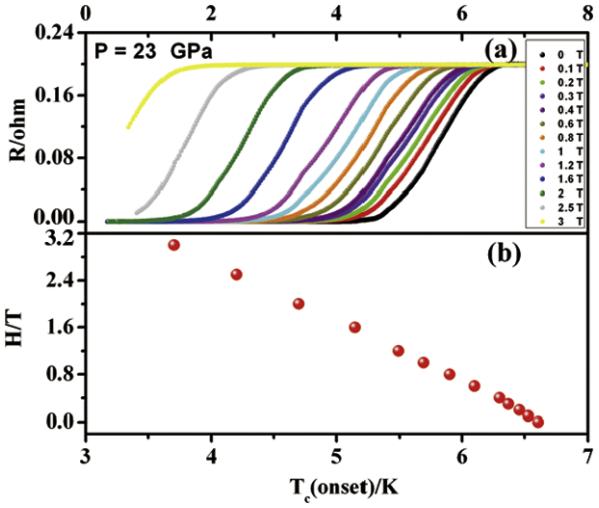

Figure 2. The superconducting transition of Bi_2Se_3 with applied magnetic field H perpendicular to the a–b plane of the single crystal at 23 GPa (a). The T_c dependence of the magnetic field H is shown in (b), and the upper critical field $H_{c2}(0)$ is extrapolated to 4.7 T at 23 GPa.

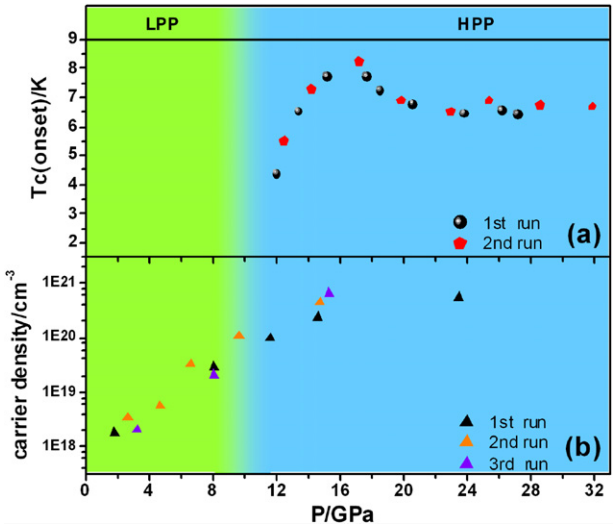

Figure 3. T_c (a) and carrier density (b) as functions of pressure from independent experiments for the low-pressure phase (LPP) and the high-pressure phase (HPP).

are similar to those reported in [20]. To confirm whether the resistance behavior is repeatable, we measured specimens from different batches. The specimen in figures 1(b) and (c) is different from that in figure 1(a). Figure 1(b) illustrates the dependence of resistance on temperature with large pressure intervals. The general trend of the resistance is metallic, semiconducting, and metallic, similar to the results of figure 1(a), as a function of pressure. We further observe clear superconducting transitions in several experiments. The results show that a drop in the resistance first occurs at around 12 GPa with a T_c of about 4.4 K. The T_c is defined using the same method as that described in [16], which is based on the differential of resistance over temperature as shown in the inset of figure 1(c). The concentration of Se vacancies can induce variations in the resistance and carrier density by several orders of magnitude at ambient pressure [22]. Different initial carrier densities could be the origin of the different resistance versus temperature curves [20]. The evolution of resistance as a function of temperature from 12.5 to 31.9 GPa is shown in figure 1(c). The value of T_c increases rapidly to a maximum of 8.2 K at 17.2 GPa as shown in the inset of figure 1(c), decreases to around 6.5 K at 23 GPa, and then remains almost constant with further increases in pressure.

To determine whether the resistive drop is indeed a superconducting transition, we measured transition temperatures at various external magnetic fields. Figure 2(a) shows the resistances measured in a low temperature range and 23 GPa with a magnetic field H applied perpendicular to the a–b plane of the single crystals. The onset transition temperature shifts toward lower temperatures by increasing H. Zero resistance disappears at higher H. This phenomenon is strong evidence that the transition is superconductive in nature. The change in H with T_c is shown in figure 2(b). Using the Werthamer–Helfand–Hohenberg formula [23], $H_{c2}(0) = -0.691 \times [\frac{dH_{c2}(T)}{dT}]_{T=T_c} \times T_c$, the upper critical field $H_{c2}(0)$ may be extrapolated to 4.7 T for magnetic field H parallel to the c axis at 23 GPa.

To demonstrate that the results are highly reproducible, we compared the results obtained from different measurements on several specimens. Figure 3 shows the dependence of T_c and carrier density on pressure. The evolution of T_c is shown in figure 3(a). According to the results from figure 3(a), we can divide the range of the pressure into two regions: the low-pressure phase and the high-pressure phases. As the pressure is increased from 12.5 to 31.9 GPa, T_c quickly increases to the maximum temperature of around 8.2 K, then decreases to nearly 6.5 K when the pressure is increased to around 23 GPa, and finally remains almost constant with further increases in pressure. Electrical transport and optical measurements show that Bi_2Se_3 is an n-type doped semiconductor [22, 24–26]. The behavior of p-type Bi_2Se_3 may be induced through slight chemical substitution [27–29]. A change of the electron state from the hole-dominated to the electron-dominated type in Bi_2Te_3 is induced by pressure, and the dependence of T_c on the pressure of Bi_2Te_3 is closely related to the change of the Hall coefficient versus pressure [30]. To study the change in carrier density in Bi_2Se_3, we performed Hall effect measurements from 2 to 23 GPa with a magnetic field H perpendicular to the a–b plane of the sample up to 7 T by sweeping the H at a fixed temperature (30 K) for each given pressure. The Hall coefficient measurements indicate that the carrier of the crystals used in the experiments is electron-dominated and does not change over the entire pressure range measured. From several measurements at ambient pressure and 30 K, we calculated the carrier density to be approximately 2×10^{18} cm^{-3}. From 2 to 23 GPa, the carrier density increases by over two orders of magnitude at 30 K, as shown in figure 3(b). Moreover, the carrier density jumps by approximately one order of magnitude at around 6.5 (around the ETT pressure) and 12 GPa (around the superconducting onset pressure). The carrier density changes quickly in the high-pressure phase.

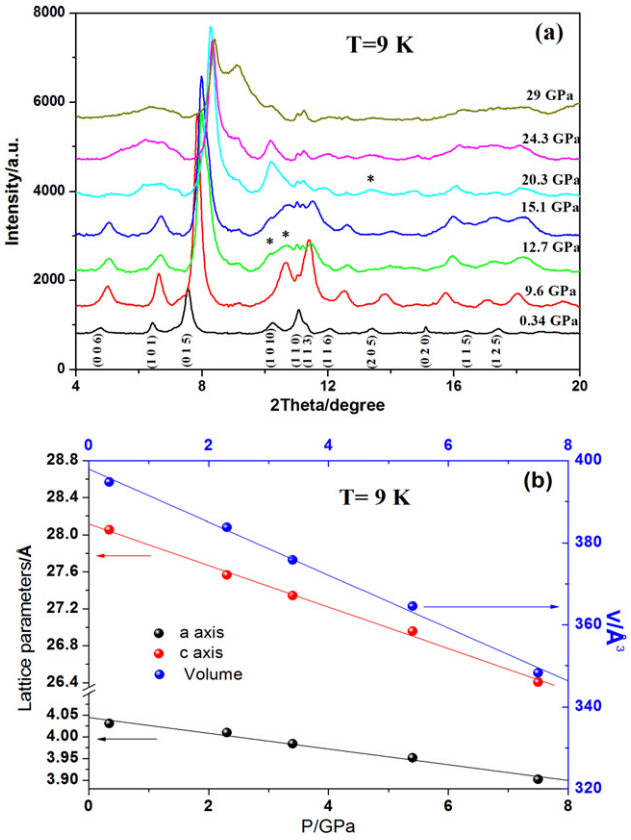

Figure 4. (a) XRD spectra of Bi_2Se_3 at different pressures at $T = 9$ K with a synchrotron radiation wavelength of 0.398 Å. The indices are assigned for the pattern at ambient pressure. Asterisks mark new peaks appearing from the high-pressure phase. (b) Lattice parameters a and c, and a plot of volume V versus pressure at 9 K. Solid lines are guides to the eye. The error bars for the experimental data are small compared to the symbols.

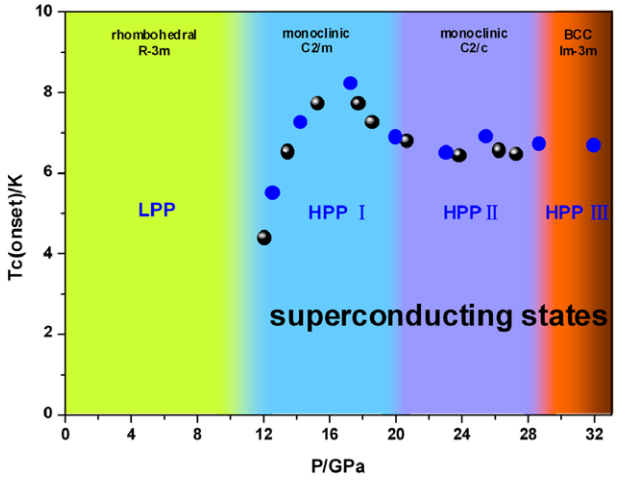

Figure 5. The phase diagram of n-type Bi_2Se_3 single crystal as a function of pressure up to 32 GPa. The black and blue balls represent superconducting transition temperatures from different experiments. LPP is for the low-pressure phase; HPP I, II and III are for high-pressure phases I, II and III, respectively.

When the carrier density rapidly increases to its maximum value, the T_c increases sharply too. Therefore, the variations in T_c with pressure are closely connected with the change in carrier density.

Compared with isostructural Bi_2Te_3, the onset pressure that induces superconductivity in Bi_2Se_3 around 12 GPa is much higher, where the high-pressure phase emerges. This could be due to the facts that the bulk energy gap of Bi_2Se_3 is almost two times that of Bi_2Te_3 and the surface Dirac point of Bi_2Se_3 is located in the direct energy gap, while that of Bi_2Te_3 is in the indirect band gap. The pressure-induced superconductivity in Bi_2Te_3 is from the low-pressure phase that keeps the Dirac surface state, while in Bi_2Se_3 the pressure-induced superconductivity is from a high-pressure phase.

To investigate the evolution of the crystal structure of Bi_2Se_3 as a function of pressure, we conducted high-pressure XRD with synchrotron radiation at 9 K, a temperature near the superconducting transition. At 9 K and pressures below 9.6 GPa, Bi_2Se_3 remains in the low-pressure phase. Further increases in pressure, however, induce a high-pressure phase. Phase transitions take place at approximately 12 and 20 GPa, as shown in figure 4(a), where new peaks marked by asterisks appear. Figure 4(b) shows the lattice parameters a and c, and a plot of volume V versus pressure in the low-pressure phase, which decreases with increasing pressure.

Referring to the results obtained from [21], we infer that Bi_2Se_3 has four phases as follows: a low-pressure phase from 0 to 12 GPa with rhombohedral $R\bar{3}m$ structure, high-pressure phase I (HPP I) from 12 to 20 GPa with monoclinic sevenfold $C2/m$ structure, high-pressure phase II (HPP II) from 20 to 29 GPa with monoclinic eightfold $C2/c$ structure, and high-pressure phase III (HPP III) above 29 GPa with BCC $Im\bar{3}m$ structure.

Figure 5 shows a global phase diagram of n-type Bi_2Se_3 single crystals as a function of pressure up to 32 GPa. According to the crystal structure phase transitions that occur at 9 K and pressures of around 12, 20, and >29 GPa, respectively, Bi_2Se_3 becomes superconducting at its high-pressure phases labeled as HPP I, HPP II and HPP III.

In summary, we found that superconductivity of Bi_2Se_3 can be achieved in its high-pressure phases. The T_c dependence of pressure is closely dependent on changes in the carrier density. XRD with synchrotron radiation further indicates four crystal structures of Bi_2Se_3 as a function of pressure with the high-pressure phases being superconducting.

This work was supported by NSF & MOST through research projects. HPSynC is supported as part of EFree, an Energy Frontier Research Center funded by the US Department of Energy under Award DE-SC0001057. HPCAT is supported by DOE-BES, DOE-NNSA (CDAC), and the National Science Foundation.

Note added in proof. During preparation of the paper (initially uploaded as arXiv:1303.0224) we learned of a similar study by K Kirshenbaum *et al* (arXiv:1302.6488).

References

[1] Bernevig B A, Hughes T L and Zhang S C 2006 *Science* **314** 1757
[2] Fu L and Kane C L 2007 *Phys. Rev.* B **76** 045302
[3] König M, Wiedmann S, Brüne C, Roth A, Buhmann H, Molenkamp L W, Qi X L and Zhang S C 2007 *Science* **318** 766
[4] Hsieh D, Qian D, Wray L, Xia Y, Hor Y S, Cava R J and Hasan M Z 2008 *Nature* **452** 970
[5] Chen Y L *et al* 2009 *Science* **325** 178
[6] Zhang H J, Liu C X, Qi X L, Dai X, Fang Z and Zhang S C 2009 *Nature Phys.* **5** 438
[7] Xia Y *et al* 2009 *Nature Phys.* **5** 398
[8] Qi X L and Zhang S C 2010 *Phys. Today* **63** 33
[9] Nayak C, Simon S H, Stern A, Freedman M and Sarma S D 2008 *Rev. Mod. Phys.* **80** 1083
[10] Qi X L and Zhang S C 2011 *Rev. Mod. Phys.* **83** 1057
[11] Larson P, Greanya V A, Tonjes W C, Liu R, Mahanti S D and Olson C G 2002 *Phys. Rev.* B **65** 085108
[12] Qi X L, Hughes T L, Raghu S and Zhang S C 2009 *Phys. Rev. Lett.* **102** 187001
[13] Fu L and Kane C L 2008 *Phys. Rev. Lett.* **100** 096407
[14] Sato T, Segawa K, Kosaka K, Souma S, Nakayama K, Eto K, Minami T, Ando Y and Takahashi T 2011 *Nature Phys.* **7** 840
[15] Hor Y S, Williams A J, Checkelsky J G, Roushan P, Seo J, Xu Q, Zandbergen H W, Yazdani A, Ong N P and Cava R J 2010 *Phys. Rev. Lett.* **104** 057001
[16] Zhang J L *et al* 2011 *Proc. Natl Acad. Sci.* **108** 24
[17] Zhang S J *et al* 2012 *J. Appl. Phys.* **111** 112630
[18] Zhang S J *et al* 2009 *Europhys. Lett.* **88** 47008
[19] Mao H K and Bell P M 1981 *Rev. Sci. Instrum.* **52** 615
[20] Hamlin J J, Jeffries J R, Butch N P, Syers P, Zocco D A, Weir S T, Vohra Y K, Paglione J and Maple M B 2012 *J. Phys.: Condens. Matter* **24** 035602
[21] Vilaplana R *et al* 2011 *Phys. Rev.* B **84** 184110
[22] Butch N P, Kirshenbaum K, Syers P, Sushkov A B, Jenkins G S, Drew H D and Paglione J 2010 *Phys. Rev.* B **81** 241301
[23] Werthamer N R, Helfand E and Hohenberg P C 1966 *Phys. Rev.* **147** 295
[24] Sushkov A B, Jenkins G S, Schmadel D C, Butch N P, Paglione J and Drew H D 2010 *Phys. Rev.* B **82** 125110
[25] Jenkins G S, Sushkov A B, Schmadel D C, Butch N P, Syers P, Paglione J and Drew H D 2010 *Phys. Rev.* B **82** 125120
[26] Cho S, Butch N P, Paglione J and Fuhrer M S 2011 *Nano Lett.* **11** 1925
[27] Kašparová J, Drašar Č, Krejčová A, Beneš L, Lošt'ák P, Chen W, Zhou Z H and Uher C 2005 *J. Appl. Phys.* **97** 103720
[28] Hor Y S, Richardella A, Roushan P, Xia Y, Checkelsky J G, Yazdani A, Hasan M Z, Ong N P and Cava R J 2009 *Phys. Rev.* B **79** 195208
[29] Choi Y H, Jo N H, Lee K J, Lee H W, Jo Y H, Kajino J, Takabatake T, Ko K-T, Park J-H and Jung M H 2012 *Appl. Phys. Lett.* **101** 152103
[30] Zhang C, Sun L L, Chen Z Y, Zhou X J, Wu Q, Yi W, Guo J, Dong X L and Zhao Z X 2011 *Phys. Rev.* B **83** 140504